

# Effects of Grape Seed-derived Polyphenols on Amyloid $\beta$ -Protein Self-assembly and Cytotoxicity<sup>\*[S]</sup>

Received for publication, August 8, 2008, and in revised form, September 17, 2008 Published, JBC Papers in Press, September 24, 2008, DOI 10.1074/jbc.M806154200

Kenjiro Ono<sup>†§1</sup>, Margaret M. Condron<sup>‡</sup>, Lap Ho<sup>¶||</sup>, Jun Wang<sup>¶</sup>, Wei Zhao<sup>¶</sup>, Giulio M. Pasinetti<sup>¶||2</sup>, and David B. Teplow<sup>†3</sup>

From the <sup>†</sup>Department of Neurology, David Geffen School of Medicine, and Molecular Biology Institute and Brain Research Institute, University of California, Los Angeles, California 90095, the <sup>‡</sup>Department of Neurology and Neurobiology and Aging, Kanazawa University Graduate School of Medical Science, Kanazawa 920-8640, Japan, the <sup>¶</sup>Department of Psychiatry and Department of Neuroscience, Mount Sinai School of Medicine, New York, New York 10029, and the <sup>||</sup>Bronx Veterans Administration Medical Center, Bronx, New York 10468

Epidemiological evidence suggests that moderate consumption of red wine reduces the incidence of Alzheimer disease (AD). To study the protective effects of red wine, experiments recently were executed in the Tg2576 mouse model of AD. These studies showed that a commercially available grape seed polyphenolic extract, MegaNatural-AZ (MN), significantly attenuated AD-type cognitive deterioration and reduced cerebral amyloid deposition (Wang, J., Ho, L., Zhao, W., Ono, K., Rosensweig, C., Chen, L., Humala, N., Teplow, D. B., and Pasinetti, G. M. (2008) *J. Neurosci.* 28, 6388–6392). To elucidate the mechanistic bases for these observations, here we used CD spectroscopy, photo-induced cross-linking of unmodified proteins, thioflavin T fluorescence, size exclusion chromatography, and electron microscopy to examine the effects of MN on the assembly of the two predominant disease-related amyloid  $\beta$ -protein alloforms, A $\beta$ 40 and A $\beta$ 42. We also examined the effects of MN on A $\beta$ -induced cytotoxicity by assaying 3-[4,5-dimethylthiazol-2-yl]-2,5-diphenyltetrazolium bromide metabolism and lactate dehydrogenase activity in A $\beta$ -treated, differentiated pheochromocytoma (PC12) cells. Initial studies revealed that MN blocked A $\beta$  fibril formation. Subsequent evaluation of the assembly stage specificity of the effect showed that MN was able to inhibit protofibril formation, pre-protofibrillar oligomerization, and initial coil  $\rightarrow$   $\alpha$ -helix/ $\beta$ -sheet secondary structure transitions.

Importantly, MN had protective effects in assays of cytotoxicity in which MN was mixed with A $\beta$  prior to peptide assembly or following assembly and just prior to peptide addition to cells. These data suggest that MN is worthy of consideration as a therapeutic agent for AD.

Alzheimer disease (AD)<sup>4</sup> has been characterized historically by the accumulation of intraneuronal filaments formed by the microtubule-associated protein tau and of extracellular parenchymal and vascular amyloid deposits largely comprising the amyloid  $\beta$ -protein (A $\beta$ ) (1). Continuing investigations of the pathogenetic relationships among tau, A $\beta$ , and AD suggest that oligomeric forms of A $\beta$  play a seminal role in disease causation (2–6). If so, the most efficacious therapeutic agents would target the assembly or neurotoxic activity of these structures. This suggestion is consistent with the fact that current AD treatments, which block brain acetylcholine degradation or *N*-methyl-D-aspartate receptors, are not preventive or curative and produce only modest and temporary symptomatic effects (7).

Nature itself already may have created useful therapeutic agents. This suggestion comes in part from the search for answers to the “French paradox,” namely that consumption of relatively large amounts of cholesterol and saturated fats occurs in the presence of decreased coronary artery disease death rates (8). Investigation of this phenomenon revealed that moderate red wine consumption might be the answer (9). The relevance of this finding to AD has come from subsequent French and Danish epidemiological studies suggesting that moderate wine drinking may protect against this disease (10–13).

Initial studies in transgenic animals of the effects of moderate consumption of red wines revealed a diminution in AD-like neuropathology and cognitive deterioration (14, 15). Recently, to establish a system enabling determination of the mechanistic basis for these epidemiologic observations, a grape seed poly-

<sup>\*</sup> This work was supported, in whole or in part, by National Institutes of Health Grant PO1 AT004511 through the NCCAM (to L. H., G. M. P., and D. B. T.) and Grant AG027818 (to D. B. T.). This work also was supported by the Department of Veterans Affairs Merit Review grant and a grant from the James J. Peters Veterans Affairs Medical Center Geriatric Research Education Clinical Center Program, and Polyphenolics (to G. M. P.); grants from the Japan Human Science Foundation and the Mochida Memorial Foundation for Medical and Pharmaceutical Research (to K. O.); and grants from the Alzheimer's Association, and the Jim Easton Consortium for Alzheimer's Drug Discovery and Biomarkers at UCLA (to D. B. T.). The costs of publication of this article were defrayed in part by the payment of page charges. This article must therefore be hereby marked “advertisement” in accordance with 18 U.S.C. Section 1734 solely to indicate this fact.

<sup>†</sup> This article was selected as a Paper of the Week.

<sup>[S]</sup> The on-line version of this article (available at <http://www.jbc.org>) contains a supplemental figure.

<sup>1</sup> Supported by a Pergolide Fellowship from Eli Lilly Japan.

<sup>2</sup> To whom correspondence may be addressed: Mount Sinai School of Medicine, 1468 Madison Ave., Rm. 14-94C, NY, NY 10029-6574. E-mail: giulio.pasinetti@mssm.edu.

<sup>3</sup> To whom correspondence may be addressed: Dept. of Neurology, 635 Charles E. Young Dr. South (Rm. 445), Los Angeles, CA 90095-7334; E-mail: dteplow@ucla.edu.

<sup>4</sup> The abbreviations used are: AD, Alzheimer disease; A $\beta$ , amyloid  $\beta$ -protein;  $\alpha$ S,  $\alpha$ -synuclein; GST, glutathione *S*-transferase; GSPE, grape seed polyphenolic extract; LMW, low molecular weight; LDH, lactate dehydrogenase; MN, MegaNatural-AZ; MTT, 3-[4,5-dimethylthiazol-2-yl]-2,5-diphenyltetrazolium bromide; NGA, NGA9–119; Ru(bpy), tris(2,2'-bipyridyl)dichlororuthenium(II); ThT, thioflavin T; Tricine, *N*-[2-hydroxy-1,1-bis(hydroxymethyl)ethyl]glycine; PICUP, photo-induced cross-linking of unmodified proteins; EM, electron microscopy; HPLC, high-performance liquid chromatography; SEC, size-exclusion chromatography.

phenolic extract (GSPE) was administered orally to Tg2576 mice, a murine model of AD (16). Significant amelioration of cognitive deficits was observed, and this amelioration correlated with reductions in the amounts of high molecular weight A $\beta$  assemblies in the brain (17). These studies support the postulation that grapes or their fermentation products contain compounds that could be useful therapeutic agents for AD.

What are these compounds? Classical biochemical fractionation studies have shown that the active components of red wine are polyphenols, including resveratrol and the proanthocyanidins (18). Resveratrol was found to lower significantly the levels of secreted and intracellular A $\beta$  produced in a variety of cell lines by increasing proteasome-mediated A $\beta$  degradation (19). Interestingly, a related polyphenolic compound, curcumin, is found in the common spice curry (20). As with red wine, epidemiologic studies have shown a correlation between curcumin (curry) consumption and decreased AD risk (21). Moreover, treatment with *Ginkgo biloba* extract EGb 761<sup>®</sup>, another polyphenol-containing preparation, has been reported to improve cognitive performance of AD patients (22). The concordance of results from these different systems emphasizes the potential importance of elucidating the mechanism through which polyphenols alter A $\beta$  aggregation and toxicity.

Initial mechanistic studies have focused on formation of large oligomers and fibrils. Wine-related polyphenols isolated by high performance liquid chromatography have been shown to inhibit the formation of A $\beta$  fibrils as well as to dissociate preformed fibrils by preferentially and reversibly binding to these structures (23–25). For example, tannic acid, myricetin, morin, and quercetin inhibited fibril formation by >70% (23, 24). Most recently, a commercially available GSPE, MegaNatural-AZ (MN), was shown to inhibit significantly the aggregation of A $\beta$  into SDS-stable high molecular weight oligomers (17).

In the studies reported here, we sought to determine how polyphenols affected A $\beta$  conformational dynamics and assembly and whether these effects correlated with peptide cytotoxicity. To do so, we treated A $\beta$ 42 and A $\beta$ 40 with MN and then monitored assembly and toxicity using a combination of CD, PICUP, ThT binding, electron microscopy (EM), MTT metabolism, and LDH activity. The results show potent inhibitory effects at all stages of peptide assembly.

## EXPERIMENTAL PROCEDURES

**Chemicals and Reagents**—Chemicals were obtained from Sigma-Aldrich Co. and were of the highest purity available. NGA9–119 (NGA) was obtained from Aurora Fine Chemicals Ltd., Graz, Austria. MegaNatural-AZ (MN) was obtained from Polyphenolics, Madera, CA. The molecular weight of catechin/epicatechin dimer, 580.6, the most abundant form of oligomer in GSPE, was used to calculate the molarity of MN. Water was produced using a Milli-Q system (Millipore Corp., Bedford, MA).

**Peptides and Proteins**—A $\beta$  peptides were synthesized, purified, and characterized as described previously (26). Briefly, synthesis was performed on an automated peptide synthesizer (model 433A, Applied Biosystems, Foster City, CA) using 9-fluorenylmethoxycarbonyl-based methods on preloaded Wang resins. Peptides were purified using reverse-phase high-perfor-

mance liquid chromatography (HPLC). Quantitative amino acid analysis and mass spectrometry yielded the expected compositions and molecular weights, respectively, for each peptide. Purified peptides were stored as lyophilizates at  $-20^{\circ}\text{C}$ . A stock solution of glutathione *S*-transferase (GST; Sigma-Aldrich) was prepared by dissolving the lyophilizate to a concentration of 250  $\mu\text{M}$  in 60 mM NaOH. Prior to use, aliquots were diluted 10-fold into 10 mM sodium phosphate, pH 7.4.

**Preparation of A $\beta$  Solutions**—Aggregate-free solutions of A $\beta$  were prepared using SEC (for a review, see Teplow (27)). The nominal monomer fraction has been termed low molecular weight (LMW) A $\beta$  because, at experimental peptide concentrations, this fraction comprises a mixture of monomer and low molecular oligomers in rapid equilibrium (28). For economy of presentation, we refer here to LMW A $\beta$  simply as “A $\beta$ .” To prepare A $\beta$ , 200  $\mu\text{l}$  of a 2 mg/ml peptide solution in dimethyl sulfoxide was sonicated for 1 min using a bath sonicator (Branson Ultrasonics, Danbury, CT) and then centrifuged for 10 min at  $16,000 \times g$ . The resulting supernate was fractionated on a Superdex 75 HR column using 10 mM phosphate buffer, pH 7.4, at a flow rate of 0.5 ml/min. The middle of the LMW peak was collected during 50 s and used immediately. A 10- $\mu\text{l}$  aliquot was taken for amino acid analysis to determine quantitatively the peptide concentration in each preparation. Typically, the concentrations of A $\beta$ 40 and A $\beta$ 42 were 30–40 and 10–20  $\mu\text{M}$ , respectively.

**Peptide Aggregation**—A $\beta$  solutions were prepared as specified above, and then 0.5-ml aliquots were placed in 1-ml microcentrifuge tubes. Test compounds were dissolved in ethanol to a final concentration of 2.5 mM and then diluted with 10 mM phosphate, pH 7.4, to produce concentrations of 10 and 50  $\mu\text{M}$ . One-half ml of each compound then was added to separate tubes of A $\beta$ , yielding final peptide concentrations of  $\sim 20$  (A $\beta$ 40) and  $\sim 10$   $\mu\text{M}$  (A $\beta$ 42) and final inhibitor concentrations of 5 and 25  $\mu\text{M}$ . Compound:peptide ratios thus were  $\sim 1:4$  (A $\beta$ 40) and  $\sim 1:2$  (A $\beta$ 42) at the lower compound concentration and 5:4 (A $\beta$ 40) and 5:2 (A $\beta$ 42) at the higher compound concentration. Control tubes with peptide alone received 0.5 ml of buffer. Control tubes with compound alone received 0.5 ml each of compound and buffer. The measured pH in all tubes was identical, 7.4, within experimental error. The tubes were incubated at  $37^{\circ}\text{C}$  for 0–10 days without agitation. We note that for each sample at each time point analyzed, aliquots used for different experiments (see below) generally all came from the same tube of A $\beta$ , ensuring that valid correlations could be made among the data thus produced.

**ThT Fluorescence**—Ten  $\mu\text{l}$  of sample was added to 190  $\mu\text{l}$  of ThT dissolved in 10 mM phosphate buffer, pH 7.4, and then the mixture was vortexed briefly. Fluorescence was determined three times at intervals of 10 s using a Hitachi F-4500 fluorometer. Excitation and emission wavelengths were 450 and 482 nm, respectively. Sample fluorescence was determined by averaging the three readings and subtracting the fluorescence of a ThT blank.

**CD Spectroscopy**—CD spectra of A $\beta$ :compound mixtures were acquired immediately after sample preparation or following 2, 3, 6, or 7 days of incubation. CD measurements were made by removing a 200- $\mu\text{l}$  aliquot from the reaction mixture,

adding the aliquot to a 1-mm path length CD cuvette (Hellma, Forest Hills, NY), and acquiring spectra in a J-810 spectropolarimeter (JASCO, Tokyo, Japan). The CD cuvettes were maintained on ice prior to introduction into the spectrometer. Following temperature equilibration, spectra were recorded at 22 °C from ~190–260 nm at 0.2 nm resolution with a scan rate of 100 nm/min. Ten scans were acquired and averaged for each sample. Raw data were manipulated by smoothing and subtraction of buffer spectra according to the manufacturer's instructions.

**Protofibril Formation**—To study protofibril formation and the effects of compounds on it, A $\beta$  was incubated according to the aggregation protocol above. Periodically during the 10-day incubation period, solutions were centrifuged at 16,000  $\times g$  for 5 min, and then 200  $\mu$ l of the supernate was fractionated by SEC at a flow rate of 0.5 ml/min on a Superdex 75 column (Amersham Biosciences) attached to a Waters 515 HPLC pump and a Waters 486 UV absorbance detector (Waters, Milford, MA), essentially as described (26). Protofibrils were detected and recovered at an elution time of ~12 min by UV absorbance at 254 nm.

**Electron Microscopy**—A 10- $\mu$ l aliquot of each sample was spotted onto a glow-discharged, carbon-coated Formvar grid (Electron Microscopy Sciences, Hatfield, PA) and incubated for 20 min. The droplet then was displaced with an equal volume of 2.5% (v/v) glutaraldehyde in water and incubated for an additional 5 min. Finally, the peptide was stained with 8  $\mu$ l of 1% (v/v) filtered (0.2  $\mu$ m) uranyl acetate in water (Electron Microscopy Sciences). This solution was wicked off, and then the grid was air-dried. Samples were examined using a JEOL CX100 transmission electron microscopy.

**Chemical Cross-linking and Determination of Oligomer Frequency Distributions**—Immediately after their preparation, samples were cross-linked using PICUP, as described (29). Briefly, to 18  $\mu$ l of protein solution were added 1  $\mu$ l of 1 mM tris(2,2'-bipyridyl)dichlororuthenium(II) (Ru(bpy)) and 1  $\mu$ l of 20 mM ammonium persulfate. The final protein:Ru(bpy):ammonium persulfate molar ratios of A $\beta$ 40 and A $\beta$ 42 were 0.29:1:20 and 0.16:1:20, respectively. The mixture was irradiated for 1 s with visible light, and then the reaction was quenched with 10  $\mu$ l of Tricine sample buffer (Invitrogen) containing 5% (v/v)  $\beta$ -mercaptoethanol. Determination of the frequency distribution of monomers and oligomers was accomplished using SDS-PAGE and silver staining, as described (29). Briefly, 20  $\mu$ l of each cross-linked sample was electrophoresed on a 10–20% gradient Tricine gel and visualized by silver staining (SilverXpress, Invitrogen). Non-cross-linked samples were used as controls in each experiment. To produce intensity profiles and calculate the relative amounts of each oligomer type, densitometry was performed, and One-Dscan software (v. 2.2.2; BD Biosciences Bioimaging) was used to determine peak areas of baseline corrected data. In some experiments, the molar amounts of Ru(bpy) and ammonium persulfate were increased, relative to peptide, by factors of 2, 5, 10, and 20.

**Cell Culture**—Rat pheochromocytoma PC12 cells were cultured in 75-cm<sup>2</sup> flasks (product number 430641, Corning Inc., Corning, NY) in F-12K medium (ATCC, Manassas, VA)

containing 15% (v/v) horse serum, 2.5% (v/v) fetal bovine serum, 100 units/ml penicillin, 0.1 mg/ml streptomycin and 25  $\mu$ g/ml amphotericin B at 37 °C in an atmosphere of 5% (v/v) CO<sub>2</sub> in air. To prepare cells for assay, the medium was removed, and the cells were washed once gently with F-12K medium containing 0.5% (v/v) fetal bovine serum, 100 units/ml penicillin, 0.1 mg/ml streptomycin, and 25  $\mu$ g/ml amphotericin B. A cell suspension then was prepared by the addition of this latter medium, but containing 100  $\mu$ g/ml nerve growth factor (Invitrogen), followed by agitation of the flask. Cell concentration was determined using trypan blue staining, after which cells were plated at a density of 30,000 cells/well (90  $\mu$ l total volume/well) in 96-well assay plates (Costar product number 3610, Corning Inc.). The nerve growth factor-induced differentiation of the cells was allowed to proceed for 48 h, at which point toxicity assays were done.

**Cytotoxicity Assays**—Toxicity was assessed in two ways. Peptides were preincubated with either 0  $\mu$ M or 25  $\mu$ M test compound in 10 mM sodium phosphate, pH 7.4, at 37 °C for 0, 2, 3, or 7 days prior to the addition of a 10- $\mu$ l aliquot of the peptide: compound mixture to the differentiated PC12 cells. Alternatively, A $\beta$  was incubated as described above but in the absence of compound. In this case, the peptide solutions were mixed with 0 or 25  $\mu$ M test compound immediately before addition to cells. Cells were treated for 24 h with a final concentration of 0 or ~2  $\mu$ M A $\beta$  alone or with A $\beta$  plus 2.5  $\mu$ M compound. Peptide: compound ratios of A $\beta$ 40 and A $\beta$ 42 were 0.72 and 0.39, respectively. In practice, the “zero time” samples for each alternative experimental procedure were equivalent, as all components were mixed with cells at the same time.

To determine toxicity, 15  $\mu$ l of MTT solution (Promega, Madison, WI) was added to each well of the microtiter plate, and the plate was incubated in the CO<sub>2</sub> incubator for an additional 3.5 h. The cells then were lysed by the addition of 100  $\mu$ l of solubilization solution (Promega, Madison, WI) followed by overnight incubation. MTT reduction was assessed by measuring absorbance at 570 nm (corrected for background absorbance at 630 nm) using a BioTek Synergy HT microplate reader (BioTek Instruments, Winooski, VT). Controls included medium with sodium phosphate (“negative”), fibrils (“positive”), and 1  $\mu$ M staurosporine (“maximal positive”). Fibrillar A $\beta$ 40 and A $\beta$ 42 were added to cells at final concentrations of 10 and 5  $\mu$ M, respectively. The same fibril preparations were used for all experiments and served to control interassay variability. To enable interassay comparisons, toxicity within each experiment was determined first. Six replicates were done for each treatment group, and the data from three independent experiments were combined and reported as mean  $\pm$  S.E. percentage of toxicity

$$T = ((A_{A\beta} - A_{\text{medium}})/(A_{\text{staurosporine}} - A_{\text{medium}})) \times 100 \quad (\text{Eq. 1})$$

where  $A_{A\beta}$ ,  $A_{\text{medium}}$ , and  $A_{\text{staurosporine}}$  were absorbance values from A $\beta$ -containing samples, medium alone, or staurosporine alone, respectively.

LDH activity was determined using the Promega (Madison, WI) CytoTox-ONE homogeneous membrane integrity assay.



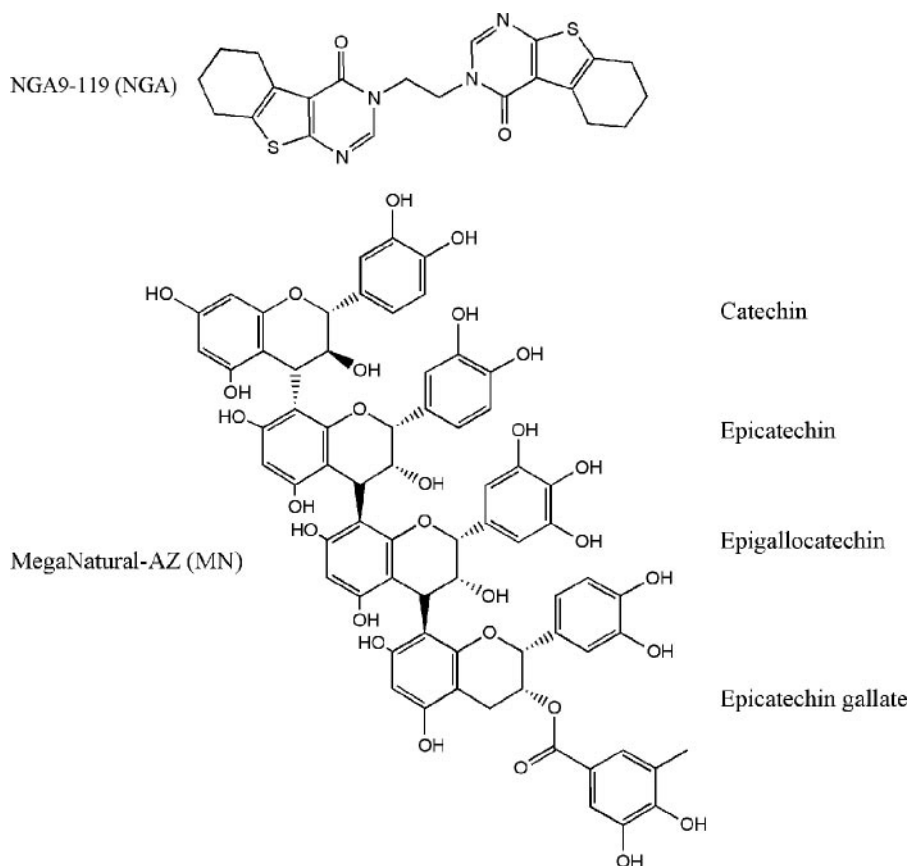


FIGURE 1. **Structures of MN and NGA.** MN is water-soluble polyphenolic extract from *Vitis vinifera* grape seeds (17). MN comprises catechin and epicatechin in monomeric (~8%), oligomeric (~75%), and polymeric (~17%) forms. The structure of a typical MN component composed of catechin and epicatechin base units and their derivatives is shown.

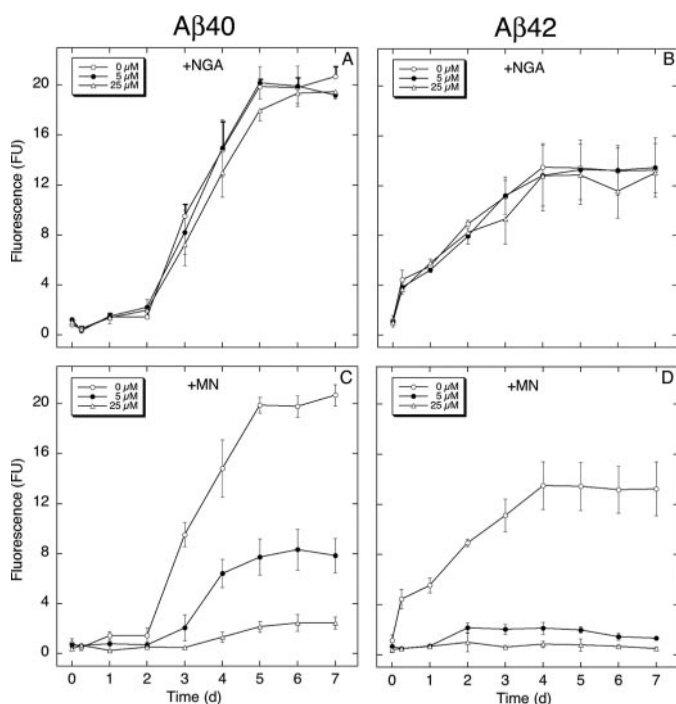


FIGURE 2. **ThT binding.** A $\beta$ 40 (A and C) or A $\beta$ 42 (B and D) were incubated for 7 days at 37 °C in 10 mM phosphate, pH 7.4, in the presence of 0 ( $\circ$ ), 5 ( $\bullet$ ), or 25 ( $\Delta$ )  $\mu$ M NGA (A and B) or MN (C and D). Periodically, aliquots were removed, and ThT binding levels were determined. Binding is expressed as mean fluorescence (in arbitrary fluorescence units (FU))  $\pm$  S.E. (error bars). Each figure comprises data obtained in three independent experiments.

To do so, peptide and peptide: compound solutions prepared as described above were incubated with the cells for 48 h. One hundred  $\mu$ l of LDH reagent then was added to each well, and the plate was incubated in the dark for 10 min, after which 50  $\mu$ l of stop solution was added and the fluorescence was measured using the BioTek Synergy HT microplate reader with excitation wavelength of 560 nm and emission wavelength of 590 nm. Controls included medium with sodium phosphate (negative), fibrils (positive), and lysis solution (maximal positive). Fibrillar A $\beta$ 40 and A $\beta$ 42 were added to cells at final concentrations of 10 and 5  $\mu$ M, respectively. Six replicates were done for each treatment group, and the data from four independent experiments were combined and reported as mean  $\pm$  S.E. The percentage of toxicity was calculated according to the formula above, except that the term  $A_{\text{staurosporine}}$  was replaced with  $A_{\text{lysis}}$ .

**Statistical Analysis**—One-way factorial analysis of variance followed by Bonferroni *post hoc* comparisons

were used to determine statistical significance among data sets. These tests were implemented within GraphPad Prism software (version 4.0a, GraphPad Software, Inc., San Diego, CA). Significance was defined as  $p < 0.05$ .

## RESULTS

Recent studies of neurological function, amyloid deposition, and peptide aggregation in the Tg2576 transgenic mouse model of AD have shown that red wine (15), and the GSPE MN (Fig. 1) (17), inhibit formation of high molecular weight SDS-stable A $\beta$  aggregates, amyloid deposition, and A $\beta$ -induced neuronal dysfunction. In the following sections, we present results of studies designed to elucidate the mechanistic bases for these inhibitory effects.

**ThT Binding**—Our first question was whether fibril formation was affected by MN. To answer this question, we used ThT to monitor temporal changes in  $\beta$ -sheet content in samples of A $\beta$ 40 and A $\beta$ 42 in the absence or presence of MN. ThT fluorescence is not a measure of fibril content *per se*, but because  $\beta$ -sheet formation correlates with fibril formation, ThT fluorescence is a useful surrogate marker (30–32). The ThT studies also allowed us to determine the kinetics of peptide assembly, providing information on nucleation and elongation phases of A $\beta$  assembly. In these and subsequent experiments, we include a medium alone control as well as a control comprising medium containing the compound NGA9–119 (Fig. 1). We include NGA here as a negative control because, like MN, it is a poly-

**TABLE 1**  
Kinetics of A $\beta$  assembly

Sample	Lag time <sup>a</sup>	Growth Rate <sup>b</sup>	Maximum intensity <sup>c</sup>
	days	FU/day	FU
A $\beta$ 40	1.6	6.1	20.7
A $\beta$ 40 + 5 $\mu$ M NGA	1.6	6.1	20.2
A $\beta$ 40 + 25 $\mu$ M NGA	1.6	5.4	19.5
A $\beta$ 40 + 5 $\mu$ M MN	1.8	2.6	8.3
A $\beta$ 40 + 25 $\mu$ M MN	2.4	0.8	2.5
A $\beta$ 42	0	2.5	13.5
A $\beta$ 42 + 5 $\mu$ M NGA	0	2.5	13.5
A $\beta$ 42 + 25 $\mu$ M NGA	0	2.3	13.1
A $\beta$ 42 + 5 $\mu$ M MN	0	1.0	2.2
A $\beta$ 42 + 25 $\mu$ M MN	>7	0	1.0

<sup>a</sup> Lag time was defined as the point of intersection with the abscissa of the line determined by the pseudo-linear portion of the fluorescence progress curve, according to Evans *et al.* (53).

<sup>b</sup> Growth rate was determined by line fitting to the pseudo-linear segment of the ascending portion of the fluorescence progress curve.

<sup>c</sup> Determined by visual inspection.

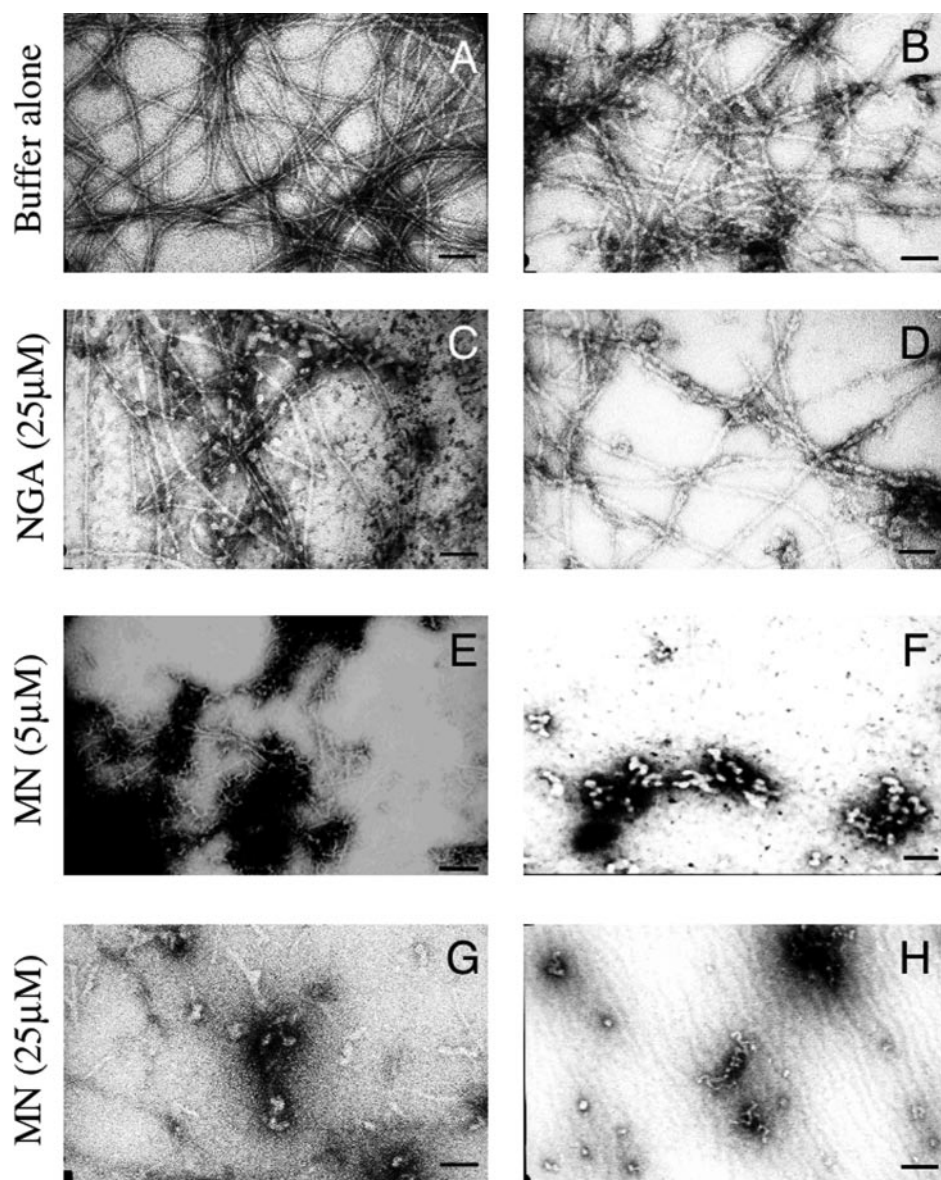


**FIGURE 3. A $\beta$  assembly morphology.** EM was used to determine the morphologies of assemblies of A $\beta$ 40 (A, C, E, and G) or A $\beta$ 42 (B, D, F, and H) incubated at 37 °C for 7 days in 10 mM sodium phosphate, pH 7.4. Peptides were incubated in buffer alone (A and B) or in the presence of 25  $\mu$ M NGA (C and D), 5  $\mu$ M MN (E and F), or 25  $\mu$ M MN (G and H). White, quasicircular structures of diameter  $\sim$ 10–30 nm were seen in some samples. These do not appear to be proteinaceous. Scale bars indicate 100 nm.

cyclic compound and thus is more representative of the composition of the MN solution than is medium alone. However, unlike MN, NGA has shown no activity in prior assays of A $\beta$  assembly.

In the absence of compounds, A $\beta$ 40 displayed a quasisigmoidal binding curve characterized by an  $\sim$ 2-day lag time, an  $\sim$ 3-day period of successively increasing ThT binding, and a binding plateau occurring after  $\sim$ 5 days (Fig. 2), results consistent with the well known nucleation-dependent polymerization model of A $\beta$  assembly (33). When A $\beta$ 40 was incubated with NGA, at a compound:peptide ratio of either 1:4 or 5:4, the binding curves were identical to that of the untreated peptide, within experimental error (Fig. 2A). In contrast, significant effects were produced by MN (Fig. 2C). These included MN concentration-dependent increases in lag time, decreases

in  $\beta$ -sheet growth rates, and decreased final  $\beta$ -sheet levels (Table 1). Almost complete inhibition of A $\beta$ 40 assembly was observed using the higher (25  $\mu$ M) MN concentration.

As with A $\beta$ 40, untreated A $\beta$ 42 and both NGA-treated samples assembled identically, within experimental error (Fig. 2B). Within the time resolution of the assay, little or no lag was observed in the development of fluorescence, which increased in a quasilinear manner for 4 days and then remained constant. When A $\beta$ 42 was incubated with MN at a compound:peptide ratio of 1:2, a 1-day lag was observed, and maximal ThT binding, which occurred 1 day later, was 6-fold lower than that of the untreated peptide (Fig. 2D; Table 1). However, at a compound:peptide ratio of 5:2, no  $\beta$ -sheet formation was observed. MN thus inhibited  $\beta$ -sheet formation by both A $\beta$ 40 and A $\beta$ 42 in a concentration-dependent manner.

**A $\beta$  Assembly Morphology**—EM was used to determine the morphologies of the A $\beta$ 40 and A $\beta$ 42 assemblies when maximal ThT binding was observed. Classical amyloid fibrils were observed in samples of untreated A $\beta$ 40 and A $\beta$ 42 (Fig. 3, A and B, respectively). The A $\beta$ 40 fibrils were non-branched, helical filaments with diameters of  $\sim$ 7 nm that exhibited a helical periodicity of  $\sim$ 220 nm. A $\beta$ 42 formed non-branched filaments of  $\sim$ 8 nm in width and with varying degrees of helicity. In addition, thicker, straight, non-branched filaments of



~12-nm-wide width were seen. Seilheimer *et al.* (34) has reported similar heterogeneity in the structure of A $\beta$ 42 fibrils *in vitro*. The addition of NGA (here for the higher, 25  $\mu$ M concentration) did not alter the assembly of either A $\beta$ 40 (Fig. 3C) or A $\beta$ 42 (Fig. 3D). In contrast to the results with NGA, strong inhibition of fibril assembly was observed in MN-treated samples at both concentrations of MN. At the lower (5  $\mu$ M) MN concentration, fibrils were seen that were thinner (4 versus 8 nm) than those formed by untreated A $\beta$  (Fig. 3E). In addition, numerous small, relatively amorphous aggregates were observed. Treatment of A $\beta$ 40 with 25  $\mu$ M MN markedly reduced fibril number and increased the relative numbers of short fibrils and amorphous aggregates (Fig. 3G). The effects of MN on A $\beta$ 42 assembly were similar in that fibril number and length were reduced greatly and the frequency of amorphous aggregates increased (Fig. 3, F and H).

**Protofibril Formation**—The immediate precursors of fibrils are protofibrils, short (<150 nm), flexible, narrow (~5 nm) assemblies often appearing as beaded chains (26, 33). To determine whether MN also affected protofibril formation, we monitored this process using SEC. As expected, incubation of A $\beta$ 40 or A $\beta$ 42 in medium alone produced chromatograms containing two predominant peaks, one eluting at ~12 min that contains protofibrils and one eluting at ~24 min that contains LMW A $\beta$  (Fig. 4A).

To enable quantitative comparisons of temporal changes in protofibril content among samples, we integrated the areas under the protofibril peaks and graphed them *versus* time (Fig. 4, B and C). Untreated A $\beta$ 40 displayed a monotonic increase in protofibril amount until plateau levels were reached at ~7 days (Fig. 4B). When A $\beta$ 40 was incubated with NGA at a compound:peptide ratio of 5:4, protofibril formation occurred with a kinetics indistinguishable from that of A $\beta$ 40 alone. In contrast, highly significant inhibition of protofibril formation was observed in the presence of MN. No significant protofibril formation was observed during the first 3 days of incubation. Thereafter, small increases in protofibril amount were observed until ~6 days, at which point the amount plateaued at a level ~7-fold lower than that of A $\beta$  alone.

Untreated A $\beta$ 42 and NGA-treated samples both formed protofibrils and did so with indistinguishable kinetics (Fig. 4C), a kinetics very similar to that of A $\beta$ 40 protofibril formation (*cf.* Fig. 4, B and C). MN almost completely blocked protofibril formation. A slight time-dependent upward trend in protofibril amount is visible (Fig. 4C), but no statistically significant differences in protofibril amount were found, relative to the amount at  $t = 0$ , at any later time points. The slightly greater inhibitory effect of MN on A $\beta$ 42 likely is due to the lower starting concentration of this A $\beta$  alloform, which resulted in an increased compound:peptide ratio.

To determine the morphologies of the assemblies present following A $\beta$  incubations with or without compounds, we examined samples after 10 days of incubation using EM. Untreated A $\beta$ 40 (Fig. 5A) and A $\beta$ 42 (Fig. 5B) produced short, relatively narrow (~7–8 nm) structures displaying periodic substructure reminiscent of “sausage links” or beaded strings, consistent with protofibril morphology (26,

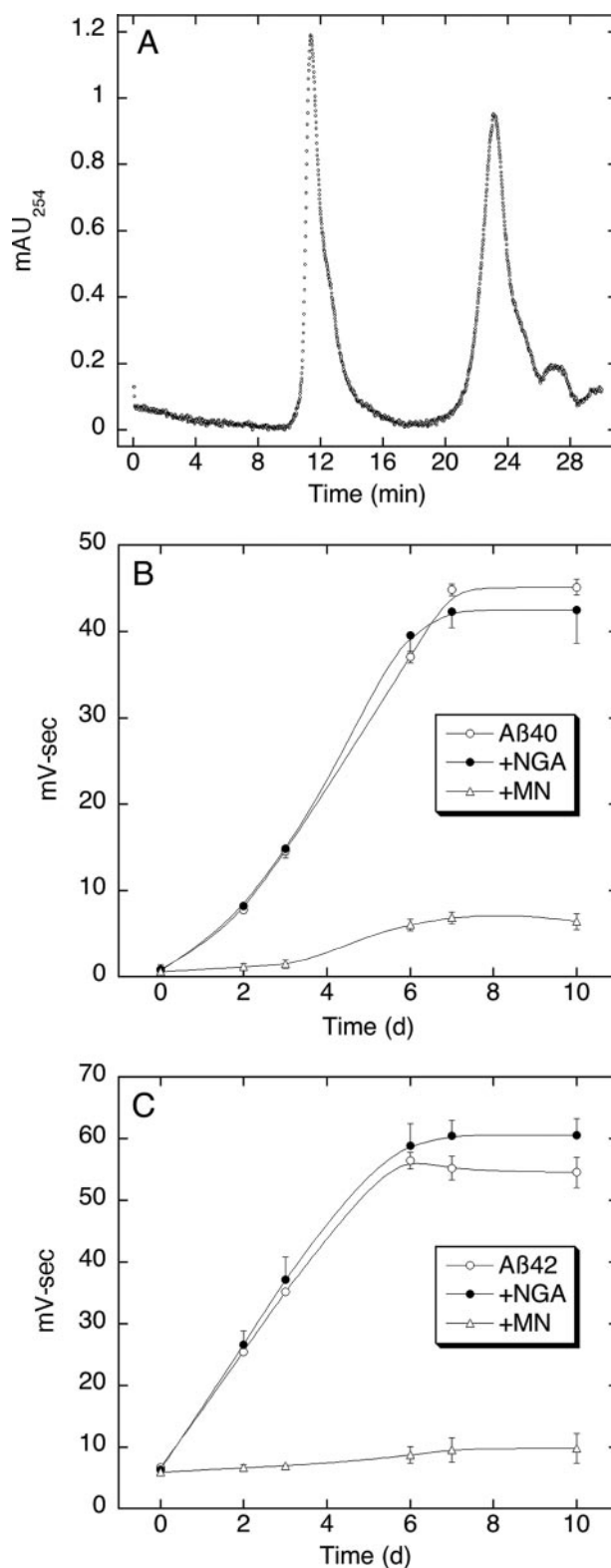


**FIGURE 4. Protofibril formation.** A $\beta$  peptides were incubated alone (○) or in the presence of 25  $\mu$ M NGA (●) or 25  $\mu$ M MN (△). Periodically during incubation, aliquots were analyzed by SEC to quantify protofibril formation. A, SEC of A $\beta$ 42 incubated alone at 37 °C for 10 days reveals a prominent protofibril peak eluting at ~12 min, along with a LMW A $\beta$  peak at ~24 min. mAU, milli-absorbance units. Similar chromatograms were obtained for A $\beta$ 40. The areas under the protofibril peaks (see A) were integrated to determine temporal changes in protofibril amounts in samples containing A $\beta$ 40 (B) or A $\beta$ 42 (C). Areas are expressed as mean area  $\pm$  S.E. (error bars). Each figure comprises data obtained in three independent experiments.

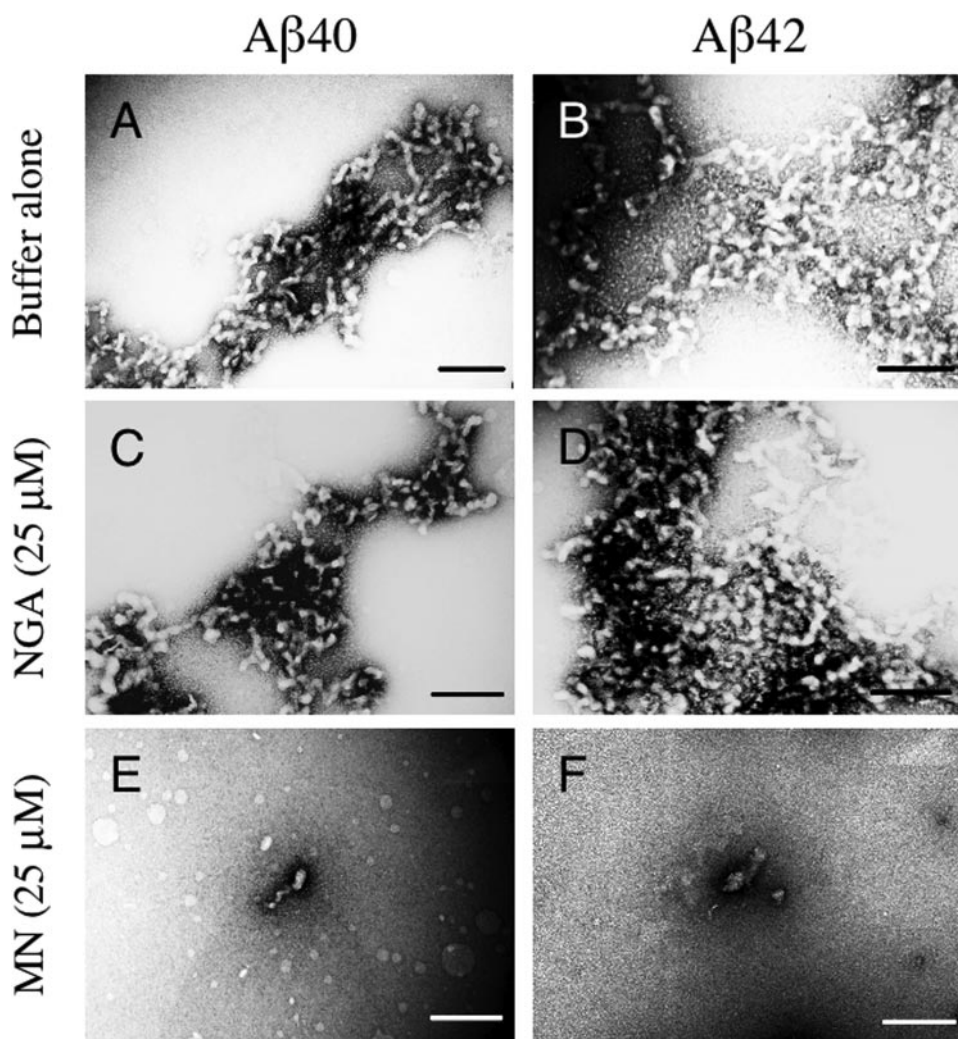


FIGURE 5. **Protofibril morphology.** EM was used to determine the morphologies of protofibrils obtained by SEC following incubation of A $\beta$ 40 (A, C, and E) or A $\beta$ 42 (B, D, and F) at 37 °C for 10 days in 10 mM sodium phosphate, pH 7.4. Peptides were incubated in buffer alone (A and B) or in the presence of 25  $\mu$ M NGA (C and D) or 25  $\mu$ M MN (E and F). Scale bars indicate 100 nm.

33). Similar structures were observed in samples that had been treated with NGA (Fig. 5, C and D). However, grids of A $\beta$ 40 or A $\beta$ 42 samples treated with MN contained few structures, and these structures were composed of fewer subunits than were structures formed in the presence of NGA or in the absence of added compounds (*cf.* Fig. 5, A–D with Fig. 5, E and F). In conclusion, these data show that MN strongly inhibits protofibril formation and that this inhibition is greatest with A $\beta$ 42.

**A $\beta$  Oligomerization.**—We next determined whether MN blocked protofibril formation by low order A $\beta$  oligomers or whether oligomerization itself was blocked. To do so, we used PICUP, a photochemical cross-linking method that is rapid, efficient, requires no structural modification of A $\beta$ , and accurately reveals the oligomerization state of A $\beta$  (for a review, see Ref. 35). In the absence of cross-linking, only A $\beta$ 40 monomers (Fig. 6A, lane 2) and A $\beta$ 42 monomers and trimers (Fig. 6B, lane 2) were observed. The A $\beta$ 42 trimer band has been shown to be an SDS-induced artifact (28, 36). Following cross-linking, and as reported previously (28), A $\beta$ 40 existed

as a mixture of monomers and oligomers of orders 2–4 (Fig. 6A, lane 3), whereas A $\beta$ 42 comprised monomers and oligomers of orders 2–6 (Fig. 6B, lane 3).

The oligomerization of A $\beta$ 40 and A $\beta$ 42 in the presence of NGA produced oligomer distributions indistinguishable from those of each peptide alone (Fig. 6, A and B, lanes 4). Increasing the compound:peptide ratio 10-fold did not alter the distribution significantly (Fig. 6, A and B, lanes 5).

When MN was mixed with A $\beta$ 40 at a compound:peptide ratio of  $\sim$ 5:4, oligomerization was blocked almost completely (Fig. 6A, lane 6). A trimer band was just visible, and the dimer intensity was very low. Increasing the compound:peptide ratio 10-fold produced similar levels of inhibition (Fig. 6A, lane 7). The effect of MN on A $\beta$ 42 oligomerization was equally significant (Fig. 6B). At compound:peptide ratios of  $\sim$ 5:2, MN produced oligomer distributions almost identical to those of untreated A $\beta$ 42, consistent with an essentially complete inhibition of oligomerization (Fig. 6B, *cf.* lanes 6 (treated) and lanes 2 (untreated)). Increasing the compound:peptide ratio 10-fold produced similar levels of inhibition (Fig. 6B, lane 7). The reader should note, as discussed above, that dissociated A $\beta$ 42 produces *both* prominent monomer

and trimer bands, whereas dissociated A $\beta$ 40 produces only monomer bands. These data show that MN can almost completely inhibit A $\beta$  oligomerization at compound:peptide ratios of  $\sim$ 5:2 or lower.

Formally, it was possible that the strong inhibition of A $\beta$  oligomerization could have resulted from an effect of the inhibitor on the PICUP chemistry itself. To evaluate this possibility, cross-linking reactions were also performed on GST ( $\sim$ 26 kDa), a positive control for the cross-linking chemistry (37). Uncross-linked GST exhibited an intense monomer band and a relatively faint dimer band (Fig. 6C, lane 2). Cross-linking produced an intense dimer band, expected because GST exists normally as a homodimer, as well as higher-order cross-linked species. No alterations in GST cross-linking were observed in the presence of NGA at either of the two compound:protein ratios tested, 1:1 (Fig. 6C, lane 4) or 10:1 (Fig. 6C, lane 5). A qualitatively similar distribution was observed with MN at a 1:1 ratio (Fig. 6C, lane 6). A significant MN effect on GST oligomerization was observed only at a 10:1 ratio, which was 4–8 times higher than the highest concentration ratio used in experi-



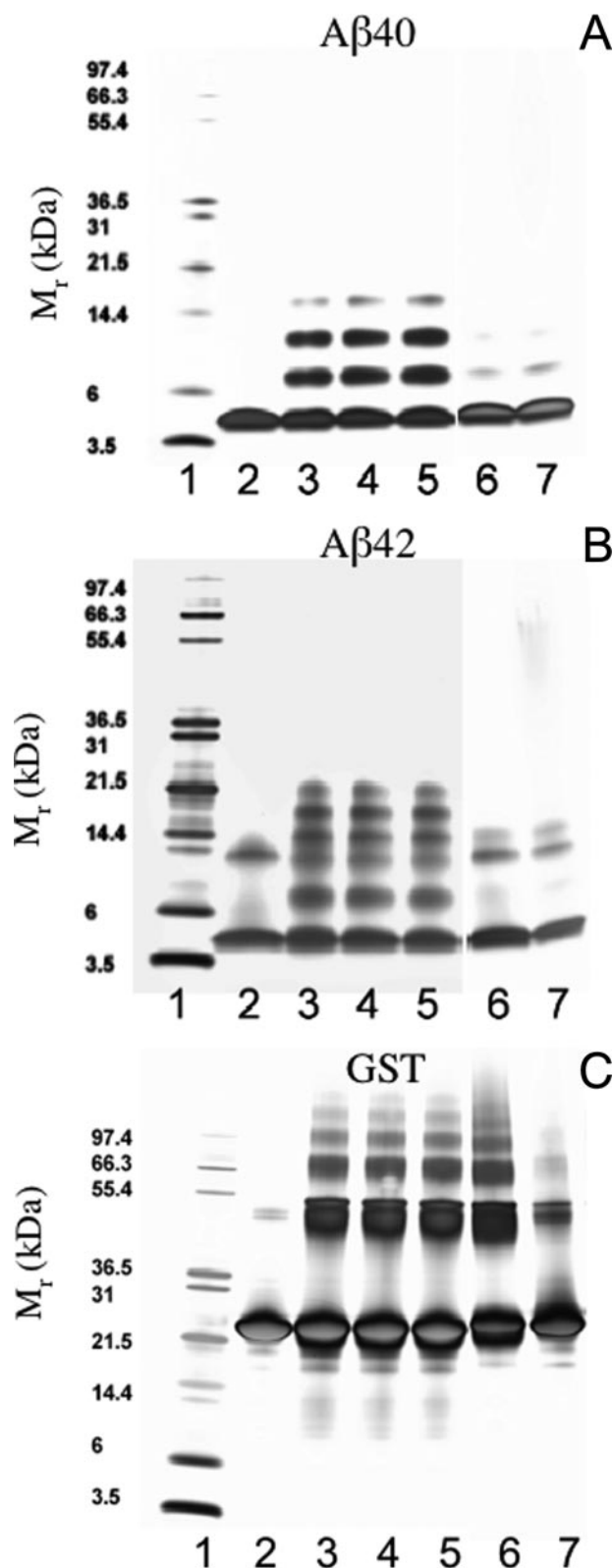


FIGURE 6. **A $\beta$  oligomerization.** PICUP, followed by SDS-PAGE and silver staining, was used to determine the effects of MN or NGA on oligomerization of A $\beta$ 40 (A), A $\beta$ 42 (B), or GST (C). Lanes 1, molecular weight markers; lanes 2, proteins alone (no cross-linking); lanes 3, proteins alone; lanes 4, proteins plus NGA (25  $\mu$ M); lanes 5, proteins plus NGA (250  $\mu$ M); lanes 6, proteins plus MN (25  $\mu$ M); and lanes 7, protein plus MN (250  $\mu$ M). Each gel is representative of each of three independent experiments.

ments with A $\beta$ . This effect may have been due to direct compound:GST effects or to effects on the chemistry. However, a chemistry effect cannot explain the strong inhibition of A $\beta$ 40 and A $\beta$ 42 oligomerization and the lack of strong inhibition of GST oligomerization, seen in Fig. 6, lanes 6 (nor inhibitory activity in other assays (see below)). We thus conclude that MN potentially inhibited both A $\beta$ 40 and A $\beta$ 42 oligomerization.

**A $\beta$  Secondary Structure Dynamics**—The oligomerization studies revealed effects of MN at the initial stages of peptide self-association. To probe the secondary structure of A $\beta$  at this stage and to determine whether MN affected later conformational properties of the peptide monomer or its oligomers, CD was used to monitor peptide assembly (Fig. 7). A $\beta$ 40 and A $\beta$ 42, incubated alone, produced initial spectra characteristic of statistical coils (Fig. 7, A and B). The major feature of these spectra was a large magnitude minimum centered at  $\sim$ 198 nm. A significant conformational transition occurred during the subsequent 3 days, producing a population comprising mixed  $\alpha$ -helix and  $\beta$ -sheet conformers. Similar conformational transitions were observed in populations of A $\beta$ 40 and A $\beta$ 42 in the presence of NGA (Fig. 7, C and D). No such transitions were observed in the presence of MN (Fig. 7, E and F). All spectra of MN-treated A $\beta$ 40 and A $\beta$ 42 revealed populations of conformers that were largely statistical coil.

We note that some variation in the absolute values of the molar ellipticities is observed among experiments. However, the inhibition of conformational changes in A $\beta$  by MN always was essentially complete and that of NGA was minimal or not observable. We also note that MN itself produces a CD spectrum (supplemental Fig. S1) with a minimum at  $\sim$ 202. The magnitude of this ellipticity does not exceed 10% of that of A $\beta$  itself. The spectrum of NGA was essentially the same as buffer alone (supplemental Fig. S1).

**Effect of Compounds on A $\beta$ -mediated Cellular Toxicity**—The ability of MN to inhibit A $\beta$  assembly suggested that it might be useful in blocking A $\beta$ -mediated cellular toxicity. To address this question, we used differentiated PC12 cells to perform MTT assays (38, 39) to probe cellular metabolism and assayed extracellular LDH activity to quantify cell death. The experimental design comprised two protocols: 1) incubating A $\beta$  with compound for various times prior to addition to cells (Fig. 8, A and B); and 2) incubating A $\beta$  without compound for various times and then mixing the compound with the A $\beta$  just prior to addition to cells (Fig. 8, C and D). The former protocol sought to determine whether pretreatment of A $\beta$ , which from our previous results should prevent peptide assembly almost entirely, blocked A $\beta$  toxicity. The latter protocol sought to determine whether compounds could block the toxicity caused by preformed A $\beta$  assemblies by binding to these assemblies and preventing their interaction with cell surface receptors. Once cells were exposed to the A $\beta$ :compound mixtures, all assays proceeded in the same manner and the data were normalized using results from cells treated with A $\beta$  fibrils, a positive control (see “Experimental Procedures”).

Previous experiments have shown that A $\beta$  fibrils tested in short incubation time assays are more toxic than LMW A $\beta$  (40). Consistent with this finding, when A $\beta$ 40 was prepared and added immediately to cells, its toxicity was  $\sim$ 20% that produced



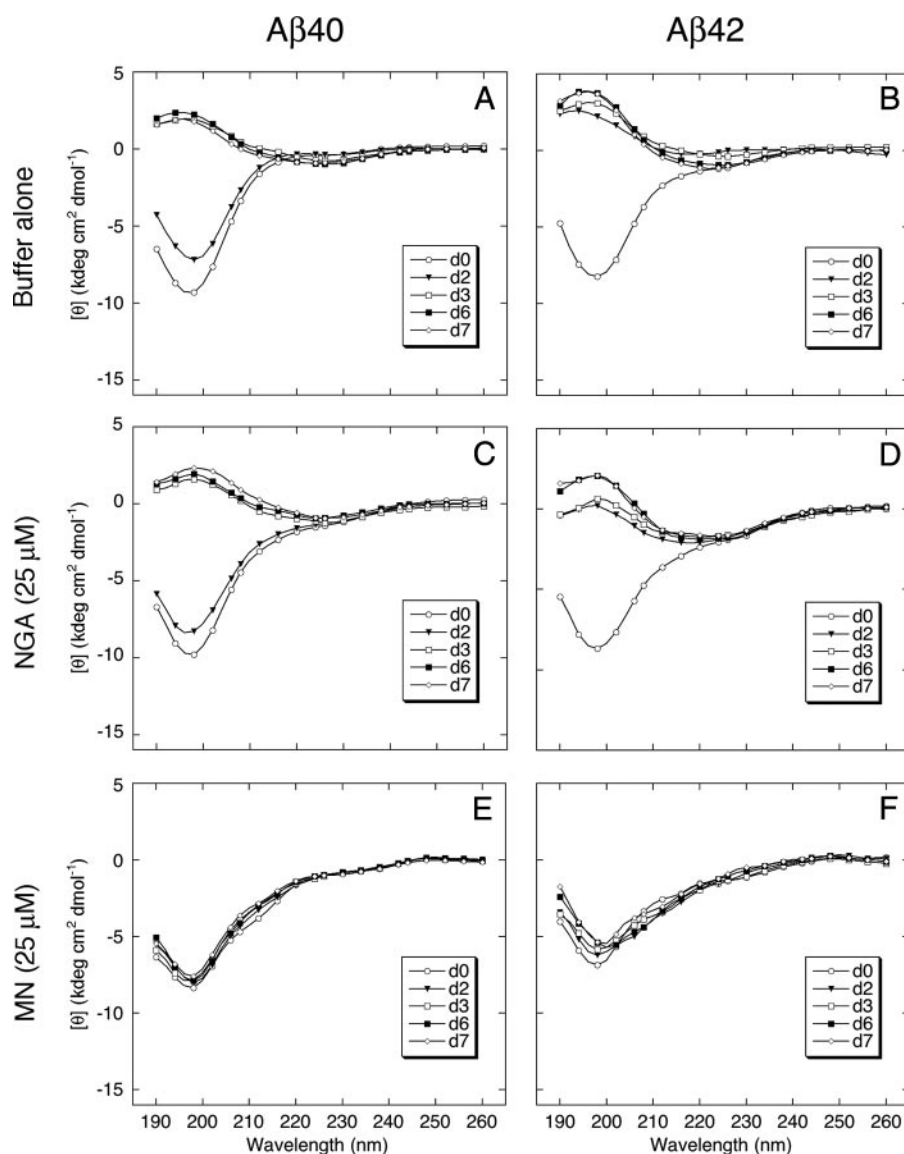


FIGURE 7. **A $\beta$  secondary structure dynamics.** A $\beta$ 40 (A, C, and E) or A $\beta$ 42 (B, D, and F) were incubated at 37 °C for 7 days in 10 mM phosphate, pH 7.4, in buffer alone (A and B) or in the presence of 25  $\mu$ M NGA (C and D) or 25  $\mu$ M MN (E and F). Spectra were acquired immediately at the start of the incubation period, day zero ( $\circ$ ), and after days 2 ( $\blacktriangledown$ ), 3 ( $\square$ ), 6 ( $\blacksquare$ ), and 7 ( $\diamond$ ). The spectra presented at each time are representative of those obtained during each of three independent experiments.

by fibrils (Fig. 8A). A $\beta$ 40 treated with NGA was equally toxic. In contrast, MN eliminated any A $\beta$ 40 toxicity. Incubation of A $\beta$ 40 for 3 days, during which time oligomers, protofibrils, and fibrils form, produced a population that was significantly more toxic. Both untreated A $\beta$ 40 and NGA-treated A $\beta$ 40 were  $\sim$ 60% toxic. Treatment of A $\beta$ 40 with MN reduced this toxicity to  $<10\%$ , which was a highly significant reduction relative to A $\beta$ 40 alone ( $p < 0.01$ ). The same qualitative relationships among the three experimental groups were observed after 7 days of incubation. Both untreated A $\beta$ 40 and NGA-treated A $\beta$ 40 were  $\sim$ 35–40% toxic, whereas MN-treated A $\beta$ 40 was  $<10\%$  toxic ( $p < 0.01$ ).

Similar observations were made in experiments with A $\beta$ 42 (Fig. 8B). Untreated and NGA-treated A $\beta$ 42 displayed similar toxicity levels at all three time points, although A $\beta$ 42 treated with NGA and immediately added to cells trended (non-signif-

icantly) toward modestly lower toxicity. MN treatment reduced A $\beta$ 42 toxicity substantially. Contemporaneous treatment eliminated toxicity, as with A $\beta$ 40, and toxicity levels were 75.7% ( $p < 0.01$ ) and 77.1% ( $p < 0.01$ ) lower at days 2 and 7, respectively.

To determine whether compounds might affect A $\beta$ -induced toxicity after peptide assembly was allowed to proceed, NGA or MN were mixed with A $\beta$ 40 or A $\beta$ 42 after the peptides had been incubated alone for various periods of time and just before addition to cells. The data thus obtained for A $\beta$ 40 (Fig. 8C) were very similar to those obtained by pretreatment (Fig. 8A). At all three incubation times, untreated and NGA-treated peptide yielded similar toxicity levels, and MN-treated peptide was either non-toxic (0 days) or substantially (64.4% (2 days) or 79.2% (7 days)) and significantly ( $p < 0.01$ ) less toxic. Qualitatively similar results were obtained in studies of A $\beta$ 42 (Fig. 8D), except that modest (14.5–17.7%) decreases of toxicity were observed in the presence of NGA at all three time points. No toxicity was observed when MN was mixed with A $\beta$ 42 and added to cells contemporaneously. Significant ( $p < 0.01$ ) decreases in toxicity were observed in MN samples treated after incubation for 2 days (38.9%) or 7 days (69.8%). The former decrease was substantially lower than that observed in the pretreated sample (75.7%), whereas the latter

decrease was the same within experimental error. In summary, for both A $\beta$ 40 and A $\beta$ 42, and for peptides that were or were not preincubated with compounds, MN was a highly effective inhibitor of A $\beta$ -induced toxicity.

We next examined the effects of compounds in the LDH assay for cell death. When A $\beta$ 40 was prepared and added immediately to cells, it was toxic, and the toxicity was  $\sim$ 40% that of fibrils (Fig. 9A). NGA-treated A $\beta$ 40 was equally toxic, whereas MN treatment decreased toxicity by  $\sim$ 61%. A $\beta$ 40 preincubated for 3 days was significantly more toxic than freshly prepared A $\beta$ . The toxicity of untreated and NGA-treated A $\beta$ 40 was equal. Treatment of A $\beta$ 40 with MN significantly ( $p < 0.01$ ) reduced this toxicity ( $\sim$ 37%). The same qualitative relationships among the three experimental groups were observed after 7 days of incubation.

Similar observations were made in experiments with untreated or pretreated A $\beta$ 42 (Fig. 9B). Untreated and NGA-

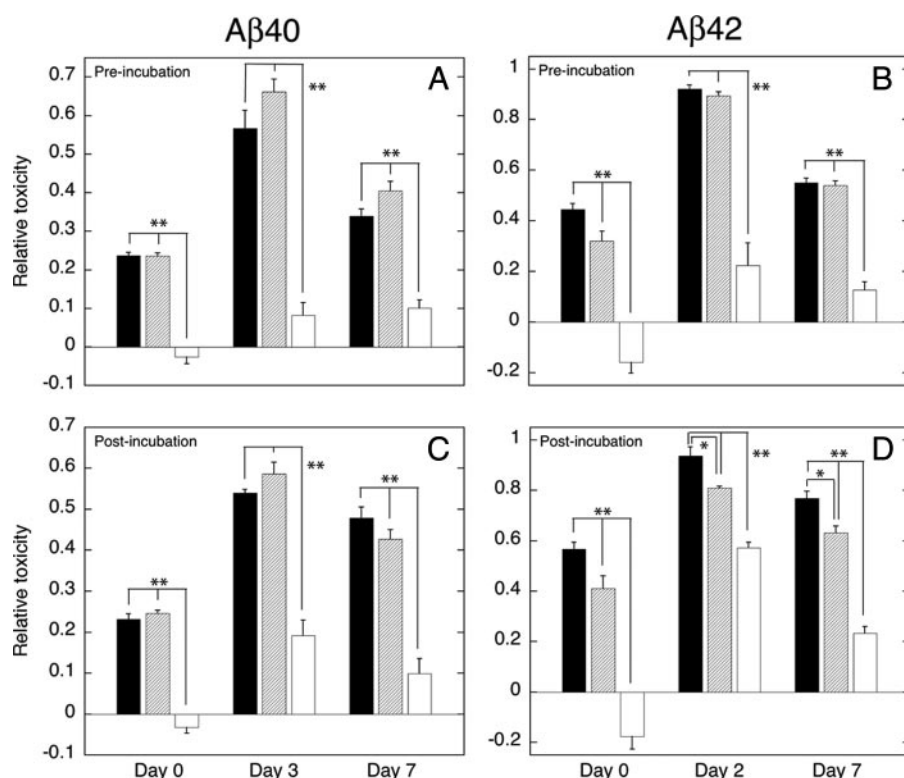


FIGURE 8. **MTT metabolism.** A $\beta$ 40 (A and C) or A $\beta$ 42 (B and D) were incubated in 10 mM sodium phosphate, pH 7.4, at 37 °C for 0, 2 (A $\beta$ 42), or 3 (A $\beta$ 40), and 7 days prior to addition to differentiated PC12 cells. In one set of experiments (A and B), the peptides were co-incubated with NGA or MN prior to addition to cells (*pre-incubation*). In a second set of experiments (C and D), NGA or MN were mixed with the peptides following the incubations (*post-incubation*) and immediately prior to addition to cells. Effects of untreated (closed bars), NGA-treated (cross-hatched bars), and MN-treated (open bars) A $\beta$  on cell metabolism were determined fluorometrically using MTT (see "Experimental Procedures") 24 h after peptide addition. A $\beta$ 40 or A $\beta$ 42 fibrils were used as a positive control and to provide a means for normalization of data among experiments. Data are presented as toxicity relative to fibrils,  $T_r$ , according to the formula  $T_r = T_{\text{sample}}/T_{\text{fibrils}}$ , where  $T_{\text{sample}}$  and  $T_{\text{fibrils}}$  are the percentage of toxicity in samples and the fibril controls, respectively (see "Experimental Procedures").  $T_r$  is presented as mean  $\pm$  S.E. (error bars). Statistical significance among groups was determined using one-way fractional analysis of variance and multiple comparison tests. Differences reaching statistical significance are noted by line segments between samples, along with their associated *p* values, where \* signifies *p* < 0.05 and \*\* signifies *p* < 0.01. Multiple comparisons show differences between buffer and MN and between NGA and MN. Unless noted, no significant differences were observed between buffer and NGA.

treated A $\beta$ 42 displayed similar toxicity levels at all three time points, and MN treatment reduced toxicity significantly (*p* < 0.05 (0 days), *p* < 0.01 (2 days), and *p* < 0.01 (7 days)). To determine whether compounds might affect A $\beta$ -induced cell lysis after peptide assembly was allowed to proceed, NGA or MN was mixed with A $\beta$ 40 or A $\beta$ 42 following incubation but just before addition to cells. The data thus obtained for A $\beta$ 40 (Fig. 9C) were very similar to those obtained by pretreatment (Fig. 9A). At all three incubation times, untreated and NGA-treated peptide yielded similar toxicity levels, and MN-treated peptide was significantly (*p* < 0.05 (0 days), *p* < 0.01 (3 days), *p* < 0.01 (7 days)) less toxic. Similar results were obtained in studies of A $\beta$ 42 (Fig. 9D). In summary, for both A $\beta$ 40 and A $\beta$ 42, and for peptides that were or were not preincubated with compounds, MN was a highly effective inhibitor of A $\beta$ -induced cell lysis.

## DISCUSSION

Polyphenols comprise a chemical class with over 8000 members, many of which are found in high concentrations in wine,

tea, nuts, berries, cocoa, and other plants (41). A substantial body of evidence suggests that polyphenols may have utility as inhibitors of fibril formation by a variety of amyloidogenic proteins (41). We have reported that wine-related polyphenols are effective inhibitors of A $\beta$ 40 and A $\beta$ 42 fibrillogenesis and that these compounds could destabilize preformed A $\beta$  aggregates (23, 24). Most recently, we reported that a GSPE, namely MN, attenuated AD-type cognitive deterioration and reduced high molecular weight soluble oligomeric A $\beta$  in the brains of Tg2576 mice (17). We sought here to examine more deeply the mechanism of inhibition, a goal critical to accelerating knowledge-based strategies for inhibitor targeting and design.

We began by studying fibril formation in parallel with assessing assembly  $\beta$ -sheet content. EM and ThT experiments revealed that MN strongly inhibited  $\beta$ -sheet and fibril formation by A $\beta$ 40 and A $\beta$ 42. Working backwards systematically along the A $\beta$  assembly pathway, we found that MN also was a highly effective inhibitor of protofibril formation and peptide oligomerization.

Early A $\beta$  structure:activity studies showed that aggregation correlated positively with cellular toxicity and that disaggregation correlated

negatively (42). Subsequent studies have sought to establish the relative importance of different types of A $\beta$  assemblies in disease pathogenesis (43). For example, protofibrils have been linked to an Arctic form of AD (44). The ability of MN to inhibit both fibril and protofibril formation suggests that it may be of value for therapeutic strategies targeting these two assembly types.

Most recently, new studies have revealed that low order oligomeric forms of A $\beta$ 42 are particularly toxic (2, 43, 45, 46). Dahlgren *et al.* (47) have shown that A $\beta$ 42 oligomers are significantly more toxic than are the homologous peptide monomers or fibrils. Consistent with this result, substantial synaptotoxicity has been observed in transgenic mice expressing high levels of A $\beta$ 42 but displaying no significant amyloid plaque pathology (48). More surprising, relative to the original amyloid cascade hypothesis (49), are recent data in transgenic animal models of AD that show that facilitating fibril formation is beneficial (4). The ability of MN to block formation of low order A $\beta$  oligomers suggests that it might also be of value for targeting what some have argued are the proximate neurotoxins in AD (2, 5, 43).



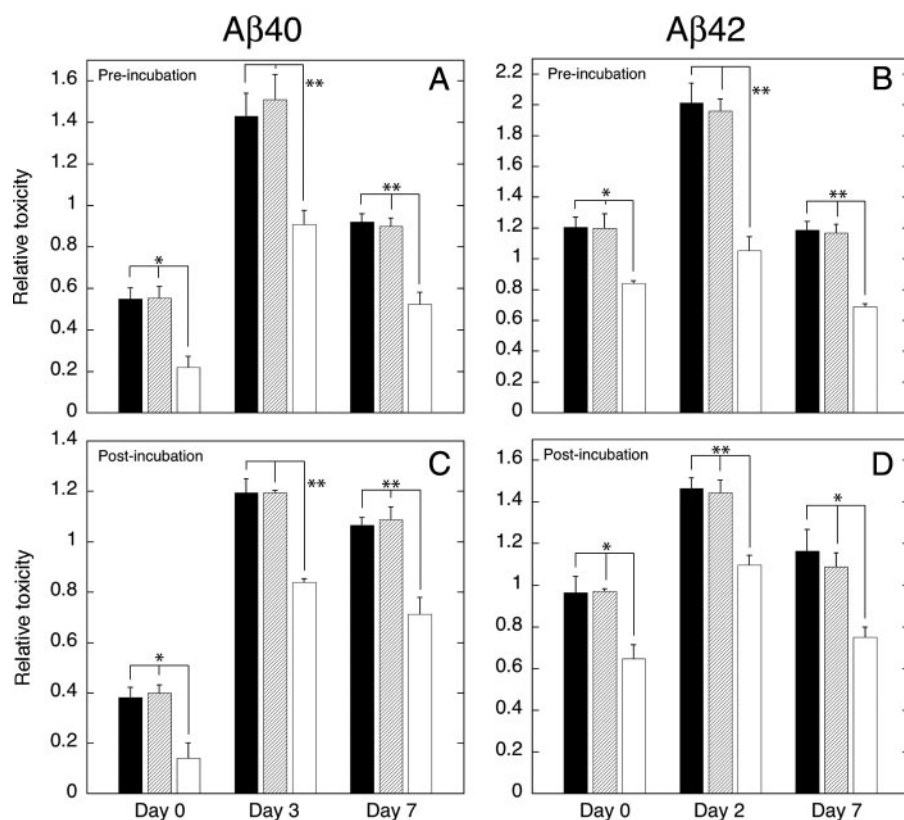


FIGURE 9. **LDH activity.** Cell death was assessed by measurement of extracellular LDH activity in samples prepared and analyzed as specified in the legend for Fig. 8 and under "Experimental Procedures." Data are presented as specified in the legend for Fig. 8.

Our CD studies, in concert with ThT experiments, showed that MN produced a conformer population comprising primarily statistical coils. Whether MN stabilizes unfolded A $\beta$  conformers or destabilizes folded conformers or oligomeric or fibrillar assemblies cannot be ascertained from the data extant. However, the consequences of MN treatment in the A $\beta$  system do appear to differ from those observed in certain other inhibitor:amyloid protein systems. For example, Zhu *et al.* (50) reported that the flavonoid baicalein stabilized a partially folded conformer of  $\alpha$ -synuclein that existed within oligomeric assemblies. Conway *et al.* (51) showed that dopamine or levodopa inhibits the fibrillization of  $\alpha$ -synuclein filaments, presumably through stabilization of  $\alpha$ -synuclein into protofibrillar structures unable to form fibrils. Taniguchi *et al.* (52) reported the formation of tau oligomers in the presence of phenothiazines, polyphenols, or porphyrins. In each of these cases, the inhibitors stabilized oligomeric states in which the respective protein maintained at least a partial fold. For A $\beta$ , this type of inhibitor activity could produce peptide populations of enhanced toxicity, if the "oligomer cascade" hypothesis is true (43). The ability of MN to block A $\beta$  monomer folding and, especially, oligomerization thus is a particularly important aspect of its mechanism of action.

The most important biological consequence of A $\beta$  self-association is the production of neurotoxic assemblies. In the work reported here, assemblies of A $\beta$ 40 and A $\beta$ 42 that were added to cultures of differentiated PC12 cells caused significant cellular damage, as measured by effects on MTT metabolism and

release of LDH through cytolysis. MN substantially reduced these toxic effects in two different experimental systems: 1) pretreatment of A $\beta$  during assembly; or 2) the contemporaneous addition of MN and preassembled peptides to cells.

Interpretation of the results in the first system is straightforward; if A $\beta$  cannot assemble, it cannot be toxic. In the second system, we speculate that three phenomena may operate: 1) complexation of A $\beta$  assemblies with MN may block binding of the assembly to the cell surface; 2) MN may disassemble the pre-existing assemblies; and 3) MN may have effects on cellular redox chemistry. Our experiments do not address these possibilities directly. However, prior work has shown that polyphenols can dissociate pre-formed fibrils and exhibit substantial anti-oxidant activity (23, 24).

In conclusion, our demonstration here of the potent inhibitory effects of MN on A $\beta$  assembly, coupled with evidence that dietary supplementation with MN attenuated AD-type cognitive deterioration and

reduced cerebral amyloid deposition in a transgenic AD mouse model (17), suggest that MN is worthy of consideration as a therapeutic agent for AD.

**Acknowledgments**—We thank Drs. Gal Bitan, Erica Fradinger, Robin Roychaudhuri, and Mohammed Inayathullah for valuable advice, critical comments, and assistance, and Margaret Condon and Clark Rosensweig for technical help.

## REFERENCES

1. Teplow, D. B. (1998) *Amyloid* **5**, 121–142
2. Klein, W. L., Stine, W. B., Jr., and Teplow, D. B. (2004) *Neurobiol. Aging* **25**, 569–580
3. Walsh, D. M., and Selkoe, D. J. (2007) *J. Neurochem.* **101**, 1172–1184
4. Cheng, I. H., Searce-Levie, K., Legleiter, J., Palop, J. J., Gerstein, H., Bien-Ly, N., Puolivali, J., Lesne, S., Ashe, K. H., Muchowski, P. J., and Mucke, L. (2007) *J. Biol. Chem.* **282**, 23818–23828
5. Haass, C., and Selkoe, D. J. (2007) *Nat. Rev. Mol. Cell Biol.* **8**, 101–112
6. Klyubin, I., Walsh, D. M., Lemere, C. A., Cullen, W. K., Shankar, G. M., Betts, V., Spooner, E. T., Jiang, L., Anwyl, R., Selkoe, D. J., and Rowan, M. J. (2005) *Nat. Med.* **11**, 556–561
7. Cummings, J. L. (2004) *N. Engl. J. Med.* **351**, 56–67
8. Ferrieres, J. (2004) *Heart (Lond.)* **90**, 107–111
9. Renaud, S., and de Lorgeril, M. (1992) *Lancet* **339**, 1523–1526
10. Letenieur, L., Dartigues, J. F., and Orgogozo, J. M. (1993) *Ann. Intern. Med.* **118**, 317–318
11. Dorozynski, A. (1997) *BMJ* **314**, 997
12. Orgogozo, J. M., Dartigues, J. F., Lafont, S., Letenieur, L., Commenges, D., Salamon, R., Renaud, S., and Breteler, M. B. (1997) *Rev. Neurol. (Paris)* **153**, 185–192

13. Truelsen, T., Thudium, D., and Gronbaek, M. (2002) *Neurology* **59**, 1313–1319
14. Wang, J., Ho, L., Zhao, Z., Seror, I., Humala, N., Dickstein, D. L., Thiyagarajan, M., Percival, S. S., Talcott, S. T., and Pasinetti, G. M. (2006) *FASEB J.* **20**, 2313–2320
15. Ho, L., Chen, L. H., Wang, J., Zhao, W., Talcott, S. T., Ono, K., Teplow, D. B., Humala, N., Cheng, A., Percival, S. S., Ferruzzi, M., Janle, E., Dickstein, D., and Pasinetti, G. (2008) *J. Alzheimer's Dis.*, in press
16. Hsiao, K., Chapman, P., Nilsen, S., Eckman, C., Harigaya, Y., Younkin, S., Yang, F. S., and Cole, G. (1996) *Science* **274**, 99–102
17. Wang, J., Ho, L., Zhao, W., Ono, K., Rosensweig, C., Chen, L., Humala, N., Teplow, D. B., and Pasinetti, G. M. (2008) *J. Neurosci.* **28**, 6388–6392
18. Flamini, R. (2003) *Mass Spectrom. Rev.* **22**, 218–250
19. Marambaud, P., Zhao, H., and Davies, P. (2005) *J. Biol. Chem.* **280**, 37377–37382
20. Sharma, R. A., Gescher, A. J., and Steward, W. P. (2005) *Eur. J. Cancer* **41**, 1955–1968
21. Ganguli, M., Chandra, V., Kamboh, M. I., Johnston, J. M., Dodge, H. H., Thelma, B. K., Juyal, R. C., Pandav, R., Belle, S. H., and DeKosky, S. T. (2000) *Arch. Neurol.* **57**, 824–830
22. Le Bars, P. L., Velasco, F. M., Ferguson, J. M., Dessain, E. C., Kieser, M., and Hoerr, R. (2002) *Neuropsychobiology* **45**, 19–26
23. Ono, K., Yoshiike, Y., Takashima, A., Hasegawa, K., Naiki, H., and Yamada, M. (2003) *J. Neurochem.* **87**, 172–181
24. Ono, K., Hasegawa, K., Naiki, H., and Yamada, M. (2004) *Biochim. Biophys. Acta* **1690**, 193–202
25. Hirohata, M., Hasegawa, K., Tsutsumi-Yasuhara, S., Ohhashi, Y., Ookoshi, T., Ono, K., Yamada, M., and Naiki, H. (2007) *Biochemistry* **46**, 1888–1899
26. Walsh, D. M., Lomakin, A., Benedek, G. B., Condron, M. M., and Teplow, D. B. (1997) *J. Biol. Chem.* **272**, 22364–22372
27. Teplow, D. B. (2006) *Methods Enzymol.* **413**, 20–33
28. Bitan, G., Kirkitadze, M. D., Lomakin, A., Vollers, S. S., Benedek, G. B., and Teplow, D. B. (2003) *Proc. Natl. Acad. Sci. U. S. A.* **100**, 330–335
29. Bitan, G., Lomakin, A., and Teplow, D. B. (2001) *J. Biol. Chem.* **276**, 35176–35184
30. LeVine, H., III (1993) *Protein Sci.* **2**, 404–410
31. LeVine, H., III (1999) *Methods Enzymol.* **309**, 274–284
32. Naiki, H., and Nakakuki, K. (1996) *Lab. Invest.* **74**, 374–383
33. Harper, J. D., and Lansbury, P. T., Jr. (1997) *Annu. Rev. Biochem.* **66**, 385–407
34. Seilheimer, B., Bohrmann, B., Bondolfi, L., Muller, F., Stuber, D., and Döbeli, H. (1997) *J. Struct. Biol.* **119**, 59–71
35. Bitan, G., and Teplow, D. B. (2004) *Acc. Chem. Res.* **37**, 357–364
36. Bitan, G., Fradinger, E. A., Spring, S. M., and Teplow, D. B. (2005) *Amyloid* **12**, 88–95
37. Fancy, D. A., and Kodadek, T. (1999) *Proc. Natl. Acad. Sci. U. S. A.* **96**, 6020–6024
38. Mosmann, T. (1983) *J. Immunol. Methods* **65**, 55–63
39. Abe, K., and Saito, H. (1998) *Neurosci. Res.* **31**, 295–305
40. Walsh, D. M., Hartley, D. M., Kusumoto, Y., Fezoui, Y., Condron, M. M., Lomakin, A., Benedek, G. B., Selkoe, D. J., and Teplow, D. B. (1999) *J. Biol. Chem.* **274**, 25945–25952
41. Porat, Y., Abramowitz, A., and Gazit, E. (2006) *Chem. Biol. Drug Des.* **67**, 27–37
42. Pike, C. J., Burdick, D., Walencewicz, A. J., Glabe, C. G., and Cotman, C. W. (1993) *J. Neurosci.* **13**, 1676–1687
43. Roychaudhuri, R., Yang, M., Hoshi, M. M., and Teplow, D. B. (October 9, 2008) *J. Biol. Chem.* 10.1074/jbc.R800036200
44. Nilsberth, C., Westlind-Danielsson, A., Eckman, C. B., Condron, M. M., Axelman, K., Forsell, C., Sten, C., Luthman, J., Teplow, D. B., Younkin, S. G., Naslund, J., and Lannfelt, L. (2001) *Nat. Neurosci.* **4**, 887–893
45. Lesné, S., Koh, M. T., Kotilinek, L., Kaye, R., Glabe, C. G., Yang, A., Gallagher, M., and Ashe, K. H. (2006) *Nature* **440**, 352–357
46. Shankar, G. M., Li, S., Mehta, T. H., Garcia-Munoz, A., Shepardson, N. E., Smith, I., Brett, F. M., Farrell, M. A., Rowan, M. J., Lemere, C. A., Regan, C. M., Walsh, D. M., Sabatini, B. L., and Selkoe, D. J. (2008) *Nat. Med.* **14**, 837–842
47. Dahlgren, K. N., Manelli, A. M., Stine, W. B., Jr., Baker, L. K., Krafft, G. A., and LaDu, M. J. (2002) *J. Biol. Chem.* **277**, 32046–32053
48. Mucke, L., Masliah, E., Yu, G. Q., Mallory, M., Rockenstein, E. M., Tatsuno, G., Hu, K., Kholodenko, D., Johnson-Wood, K., and McConlogue, L. (2000) *J. Neurosci.* **20**, 4050–4058
49. Hardy, J., and Allsop, D. (1991) *Trends Pharmacol. Sci.* **12**, 383–388
50. Zhu, M., Rajamani, S., Kaylor, J., Han, S., Zhou, F., and Fink, A. L. (2004) *J. Biol. Chem.* **279**, 26846–26857
51. Conway, K. A., Rochet, J. C., Bieganski, R. M., and Lansbury, P. T., Jr. (2001) *Science* **294**, 1346–1349
52. Taniguchi, S., Suzuki, N., Masuda, M., Hisanaga, S., Iwatsubo, T., Goedert, M., and Hasegawa, M. (2005) *J. Biol. Chem.* **280**, 7614–7623
53. Evans, K. C., Berger, E. P., Cho, C. G., Weisgraber, K. H., and Lansbury, P. T. (1995) *Proc. Natl. Acad. Sci. U. S. A.* **92**, 763–767



**Effects of Grape Seed-derived Polyphenols on Amyloid  $\beta$ -Protein Self-assembly and Cytotoxicity**

Kenjiro Ono, Margaret M. Condrón, Lap Ho, Jun Wang, Wei Zhao, Giulio M. Pasinetti and David B. Teplow

*J. Biol. Chem.* 2008, 283:32176-32187.

doi: 10.1074/jbc.M806154200 originally published online September 24, 2008

---

Access the most updated version of this article at doi: [10.1074/jbc.M806154200](https://doi.org/10.1074/jbc.M806154200)

Alerts:

- [When this article is cited](#)
- [When a correction for this article is posted](#)

[Click here](#) to choose from all of JBC's e-mail alerts

Supplemental material:

<http://www.jbc.org/content/suppl/2008/09/24/M806154200.DC1>

This article cites 52 references, 18 of which can be accessed free at <http://www.jbc.org/content/283/47/32176.full.html#ref-list-1>